



Well-width dependence of exciton-phonon scattering in In_xGa_{1-x}As/GaAs single quantum wells

Borri, Paola; Langbein, Wolfgang Werner; Hvam, Jørn Märcher; Martelli, F.

Published in:
Physical Review B

Link to article, DOI:
[10.1103/PhysRevB.59.2215](https://doi.org/10.1103/PhysRevB.59.2215)

Publication date:
1999

Document Version
Publisher's PDF, also known as Version of record

[Link back to DTU Orbit](#)

Citation (APA):
Borri, P., Langbein, W. W., Hvam, J. M., & Martelli, F. (1999). Well-width dependence of exciton-phonon scattering in In_xGa_{1-x}As/GaAs single quantum wells. *Physical Review B*, 59(3), 2215-2222. <https://doi.org/10.1103/PhysRevB.59.2215>

General rights

Copyright and moral rights for the publications made accessible in the public portal are retained by the authors and/or other copyright owners and it is a condition of accessing publications that users recognise and abide by the legal requirements associated with these rights.

- Users may download and print one copy of any publication from the public portal for the purpose of private study or research.
- You may not further distribute the material or use it for any profit-making activity or commercial gain
- You may freely distribute the URL identifying the publication in the public portal

If you believe that this document breaches copyright please contact us providing details, and we will remove access to the work immediately and investigate your claim.

Well-width dependence of exciton-phonon scattering in $\text{In}_x\text{Ga}_{1-x}\text{As}/\text{GaAs}$ single quantum wells

P. Borri, W. Langbein, and J. M. Hvam

Mikroelektronik Centret, The Technical University of Denmark, Building 345 east, DK-2800 Lyngby, Denmark

F. Martelli

Fondazione Ugo Bordon, via B. Castiglione 59, I-00142 Roma, Italy

(Received 29 April 1998)

The temperature and density dependencies of the exciton dephasing time in $\text{In}_{0.18}\text{Ga}_{0.82}\text{As}/\text{GaAs}$ single quantum wells with different thicknesses have been measured by degenerate four-wave mixing. The exciton-phonon scattering contribution to the dephasing is isolated by extrapolating the dephasing rate to zero-exciton density. From the temperature dependence of this rate we have deduced the linewidth broadening coefficients for acoustic and optical phonons. We find acoustic-phonon coefficients that increase from 1.6 to 3 $\mu\text{eV}/\text{K}$ when increasing the well width from 1 to 4 nm. This is in quantitative agreement with theoretical predictions when the spatial extension of the exciton wave function, strongly penetrating into the GaAs barrier in thin $\text{In}_x\text{Ga}_{1-x}\text{As}$ quantum wells, is taken into account. The optical-phonon coefficient does not show a systematic dependence on well thickness, and is comparable with the value for bulk GaAs. [S0163-1829(99)02103-7]

I. INTRODUCTION

The effect of phonon scattering on the exciton linewidth and dephasing time in bulk semiconductors and confined systems has attracted a lot of interest in the last 15 years. Most of the work in low-dimensional structures was dedicated to $\text{GaAs}/\text{Al}_x\text{Ga}_{1-x}\text{As}$ quantum wells (QW's).^{1,2} Full width at half maximum (FWHM) linewidth-broadening coefficients of $\sim 4 \mu\text{eV}/\text{K}$ for acoustic phonons and $\sim 17 \text{ meV}$ for optical phonons have been reported by Gammon, *et al.*² using temperature-dependent exciton linewidth analysis on $\text{GaAs}/\text{Al}_{0.3}\text{Ga}_{0.7}\text{As}$ quantum wells of different thicknesses. On the well-width dependence of these coefficients, contradictory results are reported in the literature.²⁻⁵ In the single subband approximation, an acoustic-phonon coefficient proportional to the inverse of the well width is predicted.⁵ Experimentally, a nearly constant value was found by Gammon *et al.*² and even a decreasing value when decreasing the well width is reported by Schultheis *et al.*,³ while Hillmer *et al.*⁵ measure exciton mobilities indicating an acoustic-phonon scattering that is decreasing with increasing well width.

Much less attention has been paid so far on $\text{In}_x\text{Ga}_{1-x}\text{As}/\text{GaAs}$ heterostructures, in spite of the increasing importance of these systems, for instance, for the fabrication of highly confined structures like quantum wires⁶ and quantum dots.⁷ Recently, Braun *et al.*⁸ have reported an exciton-acoustic phonon-scattering coefficient of $11 \pm 1 \mu\text{eV}/\text{K}$ in wide $\text{In}_{0.135}\text{Ga}_{0.865}\text{As}/\text{GaAs}$ quantum wires and in a two-dimensional reference quantum well of 3 nm well width. A value of $1.9 \pm 1 \mu\text{eV}/\text{K}$ was previously found by Williams *et al.*⁹ in $\text{In}_x\text{Ga}_{1-x}\text{As}/\text{GaAs}$ superlattices. An investigation on the well-width dependence of the optical-phonon coefficient has not been reported to our knowledge in these systems.

In this work, we have studied the temperature and exciton-density dependencies of the exciton dephasing time in $\text{In}_{0.18}\text{Ga}_{0.82}\text{As}/\text{GaAs}$ single quantum wells with well thick-

nesses from 1 to 4 nm, by time-integrated four-wave mixing (TI-FWM). Below 70 K the extrapolated zero-density dephasing rates show a linear temperature dependence as expected for exciton-acoustic phonon scattering. At higher temperatures, a strong increase due to longitudinal-optical (LO) phonon scattering is observed. Adding both contributions, FWHM acoustic and optical-phonon coefficients are deduced from the temperature-dependent dephasing, for all the well widths investigated. We find an increase of the acoustic-phonon coefficient from 1.6 to 3 $\mu\text{eV}/\text{K}$ with increasing well width. This is in quantitative agreement with the theoretical predictions when the effective spatial extension of the excitonic wave function in thin $\text{In}_x\text{Ga}_{1-x}\text{As}$ quantum wells is taken into account. The optical-phonon coefficient is ranging from 9 to 18 meV, comparable to the value for bulk GaAs.²

The paper is organized as follows: in Sec. II the samples and the experimental setup are described. In Sec. III, we discuss the analysis of the TI-FWM results, pointing out advantages and limits of the fitting procedure we have followed. In Sec. IV the density and temperature dependencies of the dephasing rates are discussed. In Sec. V a summary of the paper is given.

II. SAMPLES AND EXPERIMENT

The samples are grown by molecular beam epitaxy in a Varian GenII machine on (100) GaAs substrates at 520 °C. Each structure consists of two $\text{In}_{0.185}\text{Ga}_{0.815}\text{As}$ single quantum wells separated by a 100-nm-thick GaAs barrier, with well thicknesses of 1–3 nm, 1.5–4 nm, and 2–7 nm, respectively. The QW's are pseudomorphic and of good optical quality, with photoluminescence linewidths ranging from 0.7 to 3.2 meV.¹⁰ The back surfaces of all the samples have been polished in order to reduce the scattered light in the time-integrated, spectrally resolved four-wave mixing, that has

been performed in reflection geometry using two excitation pulses in the directions \mathbf{k}_1 and \mathbf{k}_2 with a tunable relative delay time τ_{12} . The laser source was a self-mode locked Ti:sapphire laser providing 100 fs pulses at 76 MHz repetition rate. The pulses were chirp compensated and spectrally shaped in a pulse shaper. The laser spectrum was centered on the heavy-hole 1s exciton resonance of the samples, avoiding to excite the heavy-hole exciton continuum, or the light-hole exciton. The FWM signal was detected in the $2\mathbf{k}_2 - \mathbf{k}_1$ direction, spatially selected by pinholes and spectrally resolved by a spectrometer and an optical multichannel analyzer with a spectral resolution of 0.2 meV.

The excited exciton densities were estimated by measuring the excitation spot size and the optical power on the sample, taking into account the surface reflection. The absorption coefficient of each well was estimated by calculating the oscillator strength¹¹ from the experimental values of the exciton-binding energies.^{12,13} The spectral overlap between laser beam and absorption line was taken into account. We have obtained exciton densities ranging from 4×10^9 to $5 \times 10^{10} \text{ cm}^{-2}$.

The polarization of the exciting beams was adjusted by Babinet-Soleil compensators, and was colinear for all the measurements reported in this paper. The samples were mounted in a helium-flow cryostat at temperatures ranging from 5 to 120 K.

III. FWM RESPONSE AND ANALYSIS

The TI-FWM traces show a dominating inhomogeneous broadening in all the samples at low temperature (5 K). In Fig. 1(a), the TI-FWM trace at the heavy-hole exciton transition in the 1.5-nm-wide well at low temperature is displayed. The FWHM homogeneous (γ) and inhomogeneous (Γ) broadenings of the sample are deduced by fitting the curve according to the expression reported by Erland *et al.*¹⁴ This expression reproduces the whole delay-time dependence of the signal for positive delay [see solid line in Fig. 1(a)] and has the form

$$I_{\text{TI-FWM}}(\omega, \tau_{12}) \propto \left| \exp \left(-\gamma \tau_{12} - 4 \ln 2 \frac{(\omega_X - \omega)^2 - (\gamma/2)^2}{\Gamma^2} \right) \times \text{erfc} \left[2 \sqrt{\ln 2} \left(\frac{\gamma}{2\Gamma} - \frac{\Gamma \tau_{12}}{8 \ln 2} + i \frac{\omega_X - \omega}{\Gamma} \right) \right] \right|^2, \quad (1)$$

where ω_X is the frequency of the exciton resonance. This formula is obtained assuming a constant dephasing time across a Gaussian inhomogeneous distribution, and infinitely short excitation pulses.

From the fit we obtain an inhomogeneous broadening nearly 20 times bigger than the homogeneous one, as indicated in the figure. Note that, when the error function becomes independent on the delay, i.e., for $\tau_{12} \gg 1/\Gamma$, an exponential decay of the FWM trace vs the delay time τ_{12} is recovered, together with a Gaussian spectrum of $I_{\text{TI-FWM}}$. In the inset of Fig. 1(a) the spectral profile at 5 ps delay time is shown (dotted curve) together with a Gaussian fit (solid curve). The resonance observed in the low-energy side of the

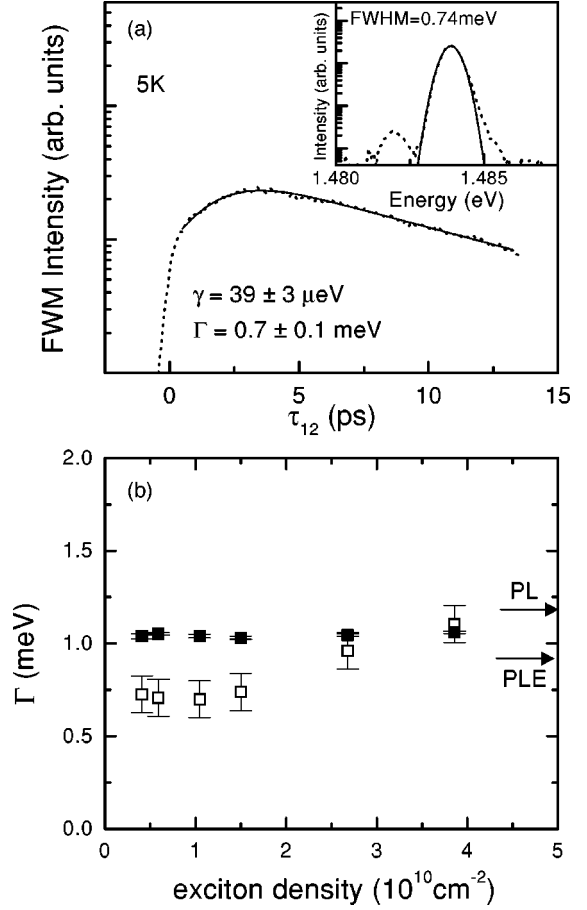


FIG. 1. (a) Delay time dependence of the FWM signal at the heavy-hole exciton transition in the 1.5-nm-wide well at 5 K. The exciton density is $1.0 \times 10^{10} \text{ cm}^{-2}$. The solid line is a fit of the experimental curve, according to Eq. (1). Homogeneous (γ) and inhomogeneous (Γ) linewidths deduced by the fit are indicated. In the inset, the spectral profile of the FWM signal at 5-ps delay is plotted (dotted line), together with a Gaussian fit (solid line). (b) Inhomogeneous linewidth vs exciton density, as deduced by fitting the spectral profile of the signal at 5-ps delay (close square) as in the inset of (a), or by fitting the delay time dependence of the FWM at the exciton resonance (open square) as in (a). For comparison, the values deduced by PL and PLE measurements in Refs. 10 and 13 are indicated as arrows.

exciton distribution is due to biexciton formation, as confirmed by its polarization dependence in the FWM experiment. The measured biexciton binding energy is 2.0 meV. The width of the FWM spectrum is smaller than the inhomogeneous linewidth by a factor of $\sqrt{2}$, according to Eq. (1). The deduced value of $\Gamma = 1.0 \text{ meV}$ is slightly larger than the one obtained by the delay dependence of the FWM. The inhomogeneous broadenings deduced by linewidth analysis of photoluminescence (PL) (Ref. 10) and photoluminescence excitation (PLE) measurements¹³ are 1.2 and 0.9 meV, respectively. In Fig. 1(b) the values of Γ as deduced by a Gaussian fit of the FWM spectrum at 5 ps delay (closed square) and by the delay dependence of the FWM signal at the exciton resonance (open square) are reported for different exciton densities. For comparison, the PL and PLE inhomogeneous broadening are indicated by the arrows. At high-exciton density the inhomogeneous broadening deduced by

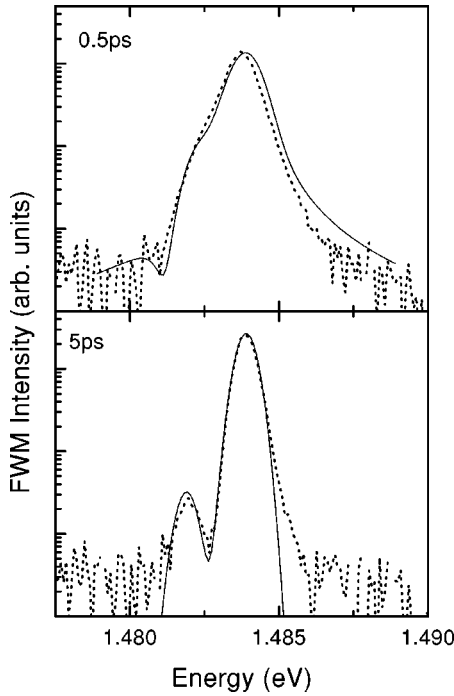


FIG. 2. FWM spectra (dotted line) at 5 K for the 1.5-nm-wide well at 0.5-ps and 5-ps delay time, respectively, at an excited exciton density of $1.0 \times 10^{10} \text{ cm}^{-2}$. The spectra at short and long delay, calculated from Eq. (1) including the biexciton resonance (Ref. 16) are also indicated as solid lines.

the delay dependence of the FWM signal is in agreement with the one obtained by the spectral profile at long delay, and a deviation within 30% is observed at low densities. Similar results are found in all the samples investigated. Deviation of the distribution from a Gaussian are small, as indicated by the spectral profiles of the FWM at long delay times, where only a small high-energy tail is observed.

A nonconstant dephasing time across the exciton distribution, not taken into account in Eq. (1), has been reported for strongly inhomogeneous broadened samples.¹⁵ In order to investigate this point, we have plotted in Fig. 2 the spectral profiles of the FWM signal (dotted line) at 0.5 ps and 5 ps delay time, for low-exciton density. In Fig. 2 the fits obtained by using Eq. (1) are also indicated as solid lines. The biexcitonic resonance has been included into the fit according to the expression reported by Langbein *et al.*¹⁶ The trace at small delay time is broader than the one at long delay as expected from Eq. (1). We conclude that the model of Erland *et al.* is in good agreement with our experimental finding, and no evidence of significantly different dephasing rates within the optically excited exciton distribution is observed.

Equation (1) is valid in the limit of nonlinearities due to phase-space filling (PSF). It is known that other nonlinearities, like excitation-induced dephasing (EID), can be a non-negligible source of FWM, modifying the delay-time dependence of the signal at positive delay in inhomogeneously broadened systems.¹⁷ In particular, in colinear polarization geometry EID has been demonstrated to be an important nonlinearity in GaAs/Al_xGa_{1-x}As multiple QW's.^{18,19} In the sample investigated here, a strong difference of the FWM intensity between colinear and cross-linear polarization of the exciting beams is also found, indicating the presence of

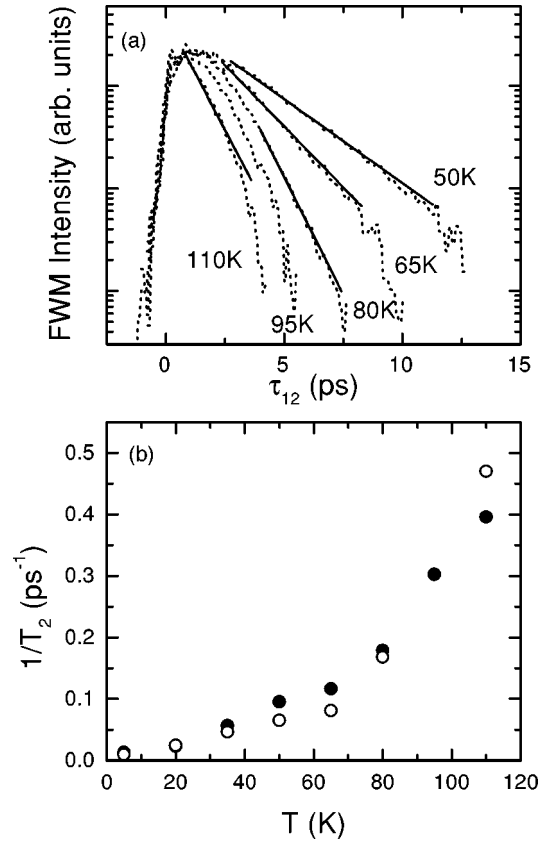


FIG. 3. (a) FWM traces vs delay time at the heavy-hole exciton transition at different temperatures in the 1.5-nm-wide well. The exciton density is $1.0 \times 10^{10} \text{ cm}^{-2}$. Exponential fits of the slopes are indicated. The FWM intensities are normalized. (b) Temperature dependence of the inverse of the dephasing rate in the 1.5-nm-wide well. The solid circle are the data obtained by fitting the FWM traces with Eq. (1), while the open circles are obtained by measuring the exponential slopes in the FWM traces as shown in (a).

EID. On the other hand, the good quality of the fits obtained with Eq. (1) and the small discrepancies reported in Fig. 1(b) indicate that this extra nonlinearity has a similar delay-time dependence as PSF. Similar results have been found in GaAs/Al_xGa_{1-x}As single quantum wells,²⁰ and explained with a delay-dependent change of the EID efficiency.

Often in literature the dephasing rate is deduced by directly measuring the exponential decay rate of the FWM trace, and dividing it by a factor of 4 when the transition is mainly inhomogeneous and the signal in real time is a photon echo, or by a factor of 2 when the transition is homogeneous and the real-time decay of the signal is a free polarization decay.¹⁷

In Fig. 3(a) the TI-FWM traces for different temperatures are shown. The FWM traces show an exponential decay at long positive delay times only for $T \leq 80 \text{ K}$; at $T = 95 \text{ K}$ the increased homogeneous broadening due to phonon scattering is comparable with the inhomogeneous one, and the traces show a nonexponential decay. For higher temperatures, the transition is mainly homogeneous and a prompt exponential decay for short positive delay appears, due to free polarization decay, while it is nonexponential for long delay time. In Fig. 3(b) we show the temperature dependence of the dephasing rate $1/T_2$ of the 1.5-nm-wide well obtained by

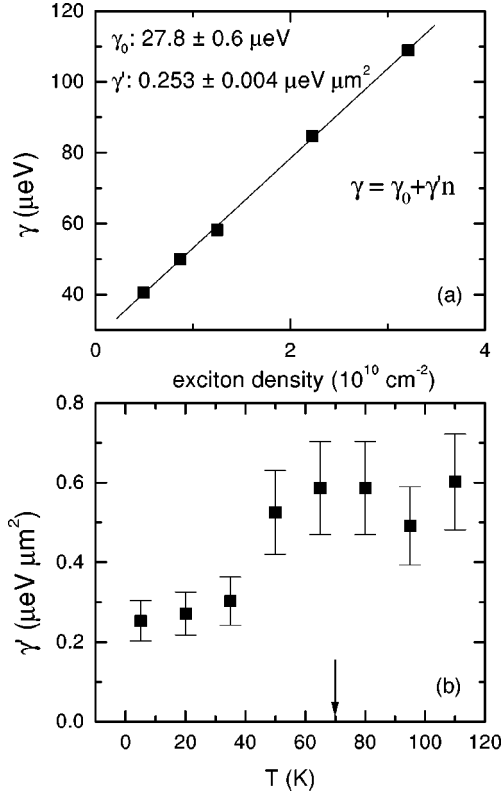


FIG. 4. (a) Density dependence of the homogeneous broadening for the 1-nm-wide well at 5 K. A linear interpolation of the data is also shown. (b) Temperature dependence of the excitation-induced dephasing coefficient. The arrow indicates the temperature at which the exciton binding energy is equal to the thermal energy $k_B T$.

performing a fit of the FWM traces according to Eq. (1) with $\gamma = 2\hbar/T_2$ (solid circles) or by using a simple exponential decay (open circles). In the latter case the FWM decay rate has been divided by 4 at low temperatures, and by 2 at higher temperatures, and the 95 K trace has been skipped. While for $T < 40 \text{ K}$ the two-fit procedures give rise to very similar results, at higher temperatures a discrepancy is found. The first fitting procedure is representing better the whole delay time dependence of the experimental data for positive delay; moreover an exponential behavior of the FWM curve is not well defined at the transition from inhomogeneous to homogeneous broadening, as shown in Fig. 3(a). We have, therefore, performed all the fits of the experimental results according to Eq. (1).

IV. TEMPERATURE AND DENSITY DEPENDENCE OF THE DEPHASING

After the discussion of the fitting procedure, in order to determine the homogeneous broadening, we now present the results. In Fig. 4(a) the density dependence of the homogeneous broadening, deduced by fitting the data as shown in Fig. 1(a), is reported for the 1-nm-wide well at 5 K. We obtain a linear dependence of γ in the range of exciton density used; the linear interpolation of the data is shown in the figure. In Fig. 4(b) the dependence of γ' (first derivative of γ with respect to the excited-exciton density) on the temperature is shown. The exciton density indicated refers to the

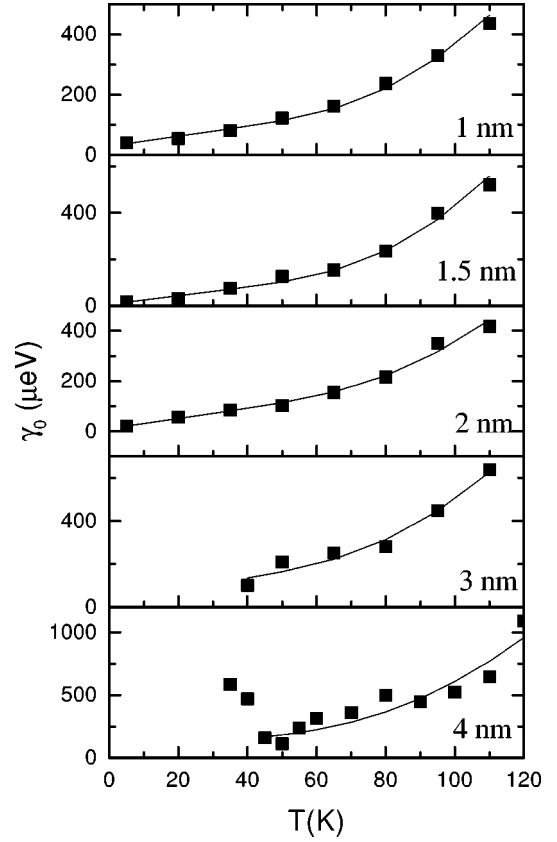


FIG. 5. Temperature dependencies of the extrapolated zero-density homogeneous broadening in all the samples investigated. The solid lines are the best fits obtained by Eq. (2).

total excited density obtained by the sum of the exciting beams. Similar results are found in all the samples investigated. In Fig. 4(b), the temperature at which the exciton binding energy is equal to the thermal-activation energy $k_B T$ is indicated with an arrow. We observe an increase of γ' for temperatures above this value, as might be expected for a higher carrier-exciton and/or carrier-carrier scattering efficiency with respect to the exciton-exciton one.

We should comment that an accurate density and temperature dependence of γ and γ' can be obtained only when the excited-exciton density is constant during the experiment, for instance in presence of a continuous-wave excitation. In our case, coherent exciton densities are created, that evolve in time. When changing the delay time between the two excited beams, different densities are probed. Moreover, if at high temperature the system is mainly homogeneous, the decay of the signal with delay time will probe the exciton density created by the first beam only, while in a photon-echo experiment the density created by the second beam is also probed.

For the purpose of this work, the results reported in Fig. 4 show that exciton-exciton scattering influences the dephasing time, and that the efficiency of this scattering depends on the temperature. Therefore, in order to isolate the contribution to the dephasing rate due to phonon-scattering, a zero-density extrapolation of the dephasing rate has been performed at each temperature. We want to comment that the results reported by Braun *et al.*⁸ and by Williams *et al.*⁹ were obtained without taking into account these effects.

In Fig. 5 the temperature dependence of the zero-density extrapolated homogeneous broadening γ_0 is reported in all the samples investigated. In the 3- and 4-nm-wide wells we have found a strong quenching of the FWM signal together with an enhancement of the dephasing rate for temperatures below 40 K. This is indicated in Fig. 5 in the case of the 4-nm well. We have, therefore, considered the results only for temperatures above 40 K, and the 7-nm-wide well has not been investigated. We can comment that these features could be explained by the presence of excess of carriers in the well that eventually bleach the absorption and increase the dephasing rate due to carrier-exciton scattering. When increasing the temperature the excess of carrier can escape from the well and a normal behavior is recovered. Anomalous features in the exciton PL of these wide wells, disappearing above 40 K, have been reported,^{21,22} indicating that the carrier distributions are influenced by photoexcitation. We want to point out that the observed behavior is not a signature of impurities, since it appears only in the wide wells, while it is not present in the thinner QW's, which are contained in the same structure.

The temperature-dependent homogeneous exciton line-width at zero density due to acoustic- and optical-phonon scattering can be expressed by²³

$$\gamma_0 = \gamma_{00} + aT + b \frac{1}{e^{\hbar\omega_{LO}/k_B T} - 1}. \quad (2)$$

The term γ_{00} is the temperature-independent contribution, aT is the acoustic-phonon contribution, which scales linearly with temperature, and the last term is due to scattering with LO phonons and is proportional to the Bose function for the LO-phonon occupation number, with the LO-phonon energy $\hbar\omega_{LO}$.

In Fig. 5 this expression has been plotted by using γ_{00} , a , and b as free parameters for the best fit with the data. Due to the small indium content in our samples, the LO-phonon energy has been fixed to the GaAs value of 36 meV. In the three wells of 1-, 1.5-, and 2-nm width we find a value of γ_{00} around 30 ± 10 μeV . This corresponds to a dephasing time T_2 of ~ 45 ps. In the literature this value is often attributed to scattering by impurities, alloy disorder, and/or interface roughness. Alloy disorder and interface roughness are responsible for the *inhomogeneous* broadening of exciton line-width, since these scattering sources are static and change the energy-level distribution. The *homogeneous* part of the line-width γ_{00} is not affected by these mechanisms. On the other hand, it has to be taken into account that, in the presence of an inhomogeneous distribution, high-energy states can have a faster dephasing rate due to the possibility of relaxation toward the lower energies by phonon emission. In this sense, alloy disorder and/or interface roughness can be a source of dephasing. In an optical experiment, we are sensitive to states in the inhomogeneous distribution with a predominant $\mathbf{K}=0$ component, which are consequently more localized. The FWM traces reported in this paper do not indicate a different dephasing rate across the exciton distribution, as already commented in the previous section. According to this result, the energy relaxation within the distribution is not expected to influence the measured γ_{00} ; instead, spin

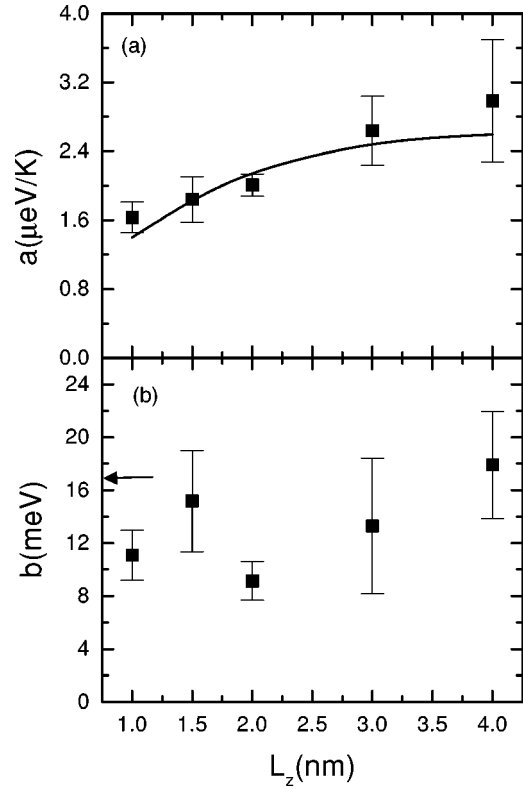


FIG. 6. (a) Well-width dependence of the acoustic-phonon coefficient. The solid line is the theoretical dependence as predicted by taking into account the spatial extension of the electron wave function into the GaAs barrier. (b) Optical-phonon coefficient as a function of the well width. The arrow indicates the GaAs bulk value reported by Gammon *et al.* (Ref. 2).

relaxation²⁴ and radiative recombination are responsible for dephasing at zero density and low temperature.

Due to the lack of experimental data at low temperatures for the 3- and 4-nm-wide wells, we have fixed $\gamma_{00} = 30$ μeV in these two samples, and used a and b as free parameters of the fit only. The results for the values of a and b are shown in Fig. 6 for all the samples. We observe an increase of the acoustic phonon coefficient when increasing the well width, while the optical-phonon coefficient shows no systematic variation.

The well-width dependence of the acoustic-phonon coefficient is given by the dependence of the spatial extension of the excitonic wave function in the growth direction. In thin $\text{In}_x\text{Ga}_{1-x}\text{As}$ QW's, the excitonic wave function penetrates significantly into the GaAs barrier (mainly due to the electron wave function), leading to a decrease of exciton binding energies and inhomogeneous linewidths, with decreasing well width.²⁵ Photoluminescence and photoluminescence-excitation measurements^{10,12} on the samples investigated here show exciton linewidths and binding energies strongly decreasing for well thicknesses below 3 nm.

We have calculated the spatial extension of electron and heavy-hole wave functions in these samples using an effective-mass model with a conduction-band offset ratio^{26,27} of 0.7 and other material parameters commonly used in literature.²⁸ In the calculation, the well width was adjusted within 10% in order to fit the experimentally observed excitonic transitions. In Fig. 7 the two electron wave

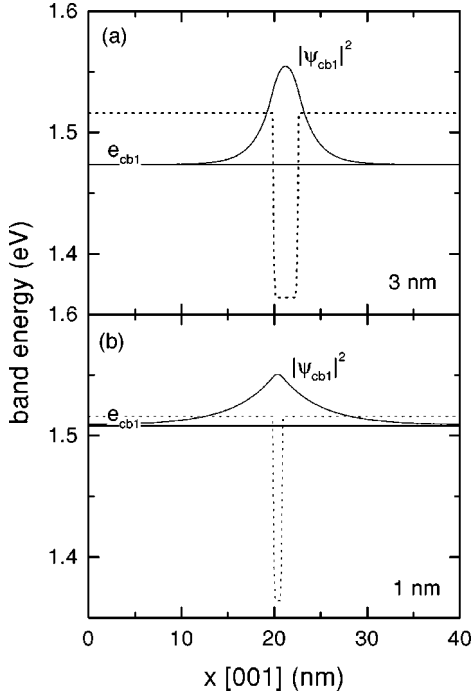


FIG. 7. (a) Spatial extension of the electron wave functions along the growth direction, calculated by using an effective mass model, for the (a) 3-nm and the (b) 1-nm-wide well. The potential profile (dotted line) and the corresponding conduction-band electronic level e_{cb1} are also indicated.

functions for the 1-nm and 3-nm-wide wells are plotted. The spatial FWHM of the square of the electron wave function (L_{ψ^2}) decreases from 7 to 4 nm when increasing the well width from 1 to 3 nm, while it is nearly constant for the 3- and 4-nm-wide wells. The hole wave function is always more confined in the well region than the electron wave function is.

In order to make a quantitative prediction of the dependence of the acoustic-phonon coefficients on the well width, we use the expression reported by Hillmer *et al.*⁵ for the exciton mobility μ due to acoustic-deformation potential scattering:

$$\mu = \frac{e\hbar^3 v_1^2 \rho L_z}{D^2 M_{\parallel}^2 k_B T}, \quad (3)$$

here e is the electron charge, v_1 is the velocity of longitudinal-acoustic (LA) phonons, ρ is the mass density, L_z is the well thickness, D is the interband hydrostatic-deformation potential,²³ and M_{\parallel} is the in-plane excitonic mass, i.e., the sum of electron and heavy-hole in-plane masses. The contribution to the linewidth due to piezoelectric interaction of electrons and holes with acoustic phonons (both LA and TA) is small compared to that from the deformation-potential interaction,²³ and, therefore, has not been included. In order to relate the mobility to the measured acoustic-phonon coefficient a we have used the following expressions:

$$aT = \frac{\hbar}{(T_1)_{\mathbf{K}=0}}, \quad (T_1)_{\mathbf{K}=0} \simeq \tau = \frac{M_{\parallel} \mu}{e}. \quad (4)$$

The first expression relates the homogeneous linewidth with the probability $1/(T_1)_{\mathbf{K}=0}$ of acoustic-phonon absorption from the optically active $\mathbf{K}=0$ state.²³ The second expression relates this transition probability with the scattering time τ for the exciton mobility.²⁹ Combining Eqs. (3) and (4) we obtain

$$a \simeq \frac{M_{\parallel} k_B D^2}{\hbar^2 v_1^2 \rho L_z}. \quad (5)$$

The scaling of the exciton-phonon scattering with the inverse of the well thickness arises from the dependence of the exciton-phonon-interaction matrix element on the phonon wave vector along the confinement direction.³⁰ Equation (3) assumes a 1s-exciton wave function formed by electrons and heavy holes belonging to the first subband of the QW, with infinite barrier potential.²⁹ The corresponding electron and hole wave functions along the confinement direction (z axis) have the form

$$f(z) = \cos(\pi z/L_z), \quad |z| < \frac{L_z}{2}. \quad (6)$$

In our case, the electron and hole wave functions are not confined into the well region only, as shown in Fig. 7. We can define then an “equivalent” well thickness \bar{L}_z with infinite barriers as the one in which the square of the wave function has the same FWHM in real space as the wave function with finite barrier (Fig. 7). According to Eq. (6), \bar{L}_z is twice the FWHM of the square of the real wave function.

Since the electron wave function is more extended into the GaAs barrier than the hole wave function, the cutoff in the overlap between acoustic phonons and exciton wave function in the interaction matrix element is dominated by the equivalent thickness of the electron wave function.³⁰ Moreover, the hole-deformation potential is about seven times smaller than that of the electron in GaAs,²⁸ therefore, the additional contribution of hole-phonon scattering at large k_z via deformation potential is negligible.

In Fig. 6(a) we have indicated as the solid curve the theoretical values of the acoustic-phonon coefficient calculated by using Eq. (5) with $L_z = 2L_{\psi^2}$. Due to the small indium content in our samples, we have used the values of v_1 , ρ , and M_{\parallel} reported by Hillmer *et al.* for GaAs. For the interband hydrostatic deformation potential, values between 7 and 10 eV are reported for GaAs.^{28,5,23} The best fit of the theoretical curve with our experimental results is found for $D = 7.8 \pm 0.5$ eV.

By assuming $L_z = 2L_{\psi^2}$ in Eq. (5) we have neglected the effect of the electron-hole Coulomb interaction in the spatial extension of the exciton wave function along the confinement direction. This can be important in the thinnest quantum well where the exciton binding energy is comparable to the confinement energies of the single carriers.¹³ There, we can expect that the single subband approximation is not applicable and the width of the excitonic wave function is

smaller than L_{ψ^2} . This corresponds to an increase of a , as also indicated by the experimental point. We can also comment that the theory used is the one commonly reported in literature, where the effect of the inhomogeneous broadening in the exciton wave function is not taken into account. When the inhomogeneous broadening is bigger than the acoustic-phonon energy, the effect of localization on the exciton wave function has certainly to be taken into account, since the interaction via acoustic phonons occurs within the inhomogeneous distribution. In the samples investigated here the inhomogeneous broadening is always smaller than $k_B T$ at 40 K; for this reason and for simplicity of discussion we have, therefore, neglected this effect.

In the investigated series of samples, the exciton-confinement energy as well as the single-carrier confinement energies change from below to above the LO-phonon energy, when increasing the well thickness. Still, we do not measure a systematic dependence of the optical-phonon coefficient on the well width, as shown in Fig. 6(b). This is in agreement with the calculations of Gammon *et al.*,² when higher subbands are available as final states, as is the case in the investigated samples. In fact, when the well width is so small to allow only one electron and hole subband, the confinement energies are also small enough to allow a transition by absorption of one LO-phonon into the GaAs barrier, while, when the confinement energies are bigger than the LO-phonon energy, more hole levels are allowed in the QW. The average value of the b coefficient is comparable with calculated and measured values of the optical-phonon coefficient in GaAs bulk reported in the literature.² We can comment that when assuming an optical-phonon coefficient independent of the well width, the fits obtained by using Eq. (2) with b as a fixed parameter equal to 14 meV are worse with respect to the ones shown in Fig. 5. This indicates that a weak

dependence of the b coefficient on the well width is actually present but not clearly resolved from our measurements due to the experimental error bars. In fact, peaked features in the predicted dependence of the optical-phonon coefficient on the well width have been reported by Gammon *et al.*² and expected to be quite weak.

V. SUMMARY

We have investigated the exciton-phonon interaction via acoustic and optical phonons by measuring the temperature dependence of the exciton dephasing rate in $\text{In}_{0.18}\text{Ga}_{0.82}\text{As}/\text{GaAs}$ single-quantum wells of different thicknesses. In order to correct for dephasing due to exciton-exciton interaction, density-dependent FWM measurements have been performed and the temperature dependence of the zero-density dephasing rate has been extracted. This dependence is in good agreement with exciton-acoustic phonon interaction via deformation potential at low temperatures and with exciton-LO phonon interaction at higher temperatures. Linewidth broadening coefficients for acoustic and optical phonons have been measured for all the samples. We have found a decreasing of the acoustic-phonon coefficient from 3 to $1.6 \mu\text{eV/K}$ when decreasing the well width from 4 to 1 nm, in agreement with theoretical predictions when the penetration of the excitonic wave function into the GaAs barrier is taken into account. The value of the optical-phonon coefficient does not show a systematic dependence on the well width within the experimental error, and it is comparable with the GaAs bulk value.

ACKNOWLEDGMENT

This work was supported by the Danish Ministries of Research and Industry in the framework of CNAST.

- ¹T. Ruf, J. Spitzer, V. F. Sapega, V. I. Belitsky, M. Cardona, and K. Ploog, *Phys. Rev. B* **50**, 1792 (1994).
- ²D. Gammon, S. Rudin, T. L. Reinecke, D. S. Katzer, and C. S. Kyono, *Phys. Rev. B* **51**, 16 785 (1995).
- ³L. Schultheis, A. Honold, J. Kuhl, K. Köhler, and C. W. Tu, *Phys. Rev. B* **34**, 9027 (1986).
- ⁴D. Oberhauser, K.-H. Pantke, J. M. Hvam, G. Weimann, and C. Klingshirn, *Phys. Rev. B* **47**, 6827 (1993).
- ⁵H. Hillmer, A. Forchel, S. Hansmann, M. Morohashi, E. Lopez, H. P. Meier, and K. Ploog, *Phys. Rev. B* **39**, 10 901 (1989).
- ⁶R. Rinaldi, R. Cingolani, L. DeCaro, M. Lomascolo, M. DiDio, L. Tapfer, U. Marti, and F. K. Reinhart, *J. Opt. Soc. Am. B* **13**, 1031 (1996).
- ⁷D. Bimberg, N. N. Ledentsov, M. Grundmann, N. Kirstaedter, O. G. Schmidt, M. H. Mao, V. M. Ustinov, A. Y. Egorov, A. E. Zhukov, P. S. Kopev, Z. I. Alferov, S. S. Ruvimov, U. Gösele, and J. Heydenreich, *Phys. Status Solidi B* **194**, 159 (1996).
- ⁸W. Braun, M. Bayer, A. Forchel, H. Zull, J. P. Reithmaier, A. I. Filin, and T. L. Reinecke, *Phys. Rev. B* **56**, 12 096 (1997).
- ⁹G. V. M. Williams, C. C. Phillips, and K. Woodbridge, *Semicond. Sci. Technol.* **9**, 1096 (1994).
- ¹⁰A. Patané, A. Polimeni, M. Capizzi, and F. Martelli, *Phys. Rev. B* **52**, 2784 (1995).
- ¹¹L. C. Andreani, in *Confined Electrons and Photons: New Physics and Devices*, edited by E. Burstein and C. Weisbuch (Plenum Press, New York, 1994).
- ¹²D. Orani, A. Polimeni, A. Patané, M. Capizzi, F. Martelli, A. D'Andrea, N. Tomassini, P. Borri, M. Gurioli, and M. Colocci, *Phys. Status Solidi A* **164**, 107 (1997).
- ¹³P. Borri, Ph.D. thesis, University of Florence, 1997.
- ¹⁴J. Erland, K. H. Pantke, V. Mizeikis, V. G. Lyssenko, and J. M. Hvam, *Phys. Rev. B* **50**, 15 047 (1994).
- ¹⁵M. Koch, D. Weber, J. Feldmann, E. O. Göbel, T. Meier, A. Schulze, P. Thomas, and S. Schmitt-Rink, *Phys. Rev. B* **47**, 1532 (1993).
- ¹⁶W. Langbein, J. M. Hvam, M. Umlauff, H. Kalt, B. Jobst, and D. Hommel, *Phys. Rev. B* **55**, R7383 (1997).
- ¹⁷J. Shah, *Ultrafast Spectroscopy of Semiconductors and Semiconductor Nanostructures* (Springer, Berlin, 1996), Chap. 2.
- ¹⁸Y. Z. Hu, R. Binder, S. W. Koch, S. T. Cundiff, H. Wang, and D. G. Steel, *Phys. Rev. B* **49**, 14 382 (1994).
- ¹⁹P. Borri, W. Langbein, D. Birkedal, V. G. Lyssenko, and J. M. Hvam, *Phys. Status Solidi A* **164**, 61 (1997).
- ²⁰W. Langbein, P. Borri, and J. M. Hvam, *International Quantum Electronics Conference (IQEC'98)*, Technical Digest Vol. 7 (Optical Society of America, 1998), p. 103.

- ²¹P. Borri, M. Gurioli, M. Colocci, F. Martelli, M. Capizzi, A. Patanè, and A. Polimeni, J. Appl. Phys. **80**, 3011 (1996).
- ²²F. Martelli, A. Polimeni, A. Patanè, M. Capizzi, P. Borri, M. Gurioli, M. Colocci, A. Bosacchi, and S. Franchi, Phys. Rev. B **53**, 7421 (1996).
- ²³S. Rudin, T. L. Reinecke, and B. Segall, Phys. Rev. B **42**, 11 218 (1990).
- ²⁴R. E. Worsley, N. J. Traynor, T. Grevatt, and R. T. Harley, Phys. Rev. Lett. **76**, 3224 (1996).
- ²⁵J. P. Reithmaier, R. Höger, and H. Riechert, Phys. Rev. B **43**, 4933 (1991).
- ²⁶J. Barnes, J. Nelson, K. W. J. Barnham, J. S. Roberts, M. A. Pate, R. Grey, S. S. Dosanjh, M. Mazzer, and F. Ghirardo, J. Appl. Phys. **79**, 7775 (1996).
- ²⁷J.-Y. Marzin, M. N. Charasse, and B. Sermage, Phys. Rev. B **31**, 8298 (1985).
- ²⁸*Landolt-Börnstein, Numerical Data and Functional Relationships in Science and Technology*, edited by O. Madelung, New Series, Group III, Vol. 22, Pt. a (Springer, Berlin, 1987).
- ²⁹P. K. Basu and Partha Ray, Phys. Rev. B **44**, 1844 (1991).
- ³⁰C. Piermarocchi, F. Tassone, V. Savona, A. Quattropani, and P. Schwendimann, Phys. Rev. B **53**, 15 834 (1996).